Article:

He, H., Chang, S., Feng, W. et al. (2026) Lagged ENSO teleconnection mechanisms driving Antarctic stratospheric ozone depletion variability. Atmospheric Research, 329. 108539. ISSN: 0169-8095

https://doi.org/10.1016/j.atmosres.2025.108539

Highlights

- ENSO peak affects Antarctic spring stratospheric ozone in the next year.
- El Niño reduces Antarctic spring ozone depletion in the decaying year.
- Tropical SST anomalies alters Brewer-Dobson circulation via upward planetary wave propagation.

Lagged ENSO Teleconnection Mechanisms Driving Antarctic Stratospheric Ozone Depletion Variability

Haotian He [a], Shujie Chang [a, b, *], Wuhu Feng [b, c], Martyn P. Chipperfield [b, d], Sandip S. Dhomse [b, d], Yuwen Li [b, e], Saffron Heddell [b]

[a] College of Ocean and Meteorology, Laboratory for Coastal Ocean Variation and Disaster Prediction, College of Ocean and Meteorology, Key Laboratory of Climate Resources and Environment in Continental Shelf Sea and Deep Ocean (LCRE), Key Laboratory of Space Ocean Remote Sensing and Application, Ministry of Natural Resources, Guangdong Ocean University, Zhanjiang, China

[b] School of Earth and Environment, University of Leeds, Leeds, UK

[c] National Centre for Atmospheric Science (NCAS), University of Leeds, Leeds, UK

[d] National Centre for Earth Observation (NCEO), University of Leeds, Leeds, UK

[e] School of Atmospheric Sciences, Nanjing University, Nanjing, China

* Corresponding author.

E-mail address: changsj@gdou.edu.cn (Shujie Chang)

Highlights

- ENSO peak affects Antarctic spring stratospheric ozone in the next year.
- El Niño reduces Antarctic spring ozone depletion in the decaying year.
- Tropical SST anomalies alters Brewer-Dobson circulation via upward planetary wave propagation.

Abstract

The interaction between the El Niño-Southern Oscillation (ENSO) and Antarctic stratospheric ozone represents an important tropical-polar coupling mechanism. Using satellite-based observations, reanalysis datasets, and simulations from the global three-dimensional chemical-transport (TOMCAT) and chemistry-climate (WACCM) models, this study investigates how sea surface temperature anomalies (SSTA) associated with ENSO influence ozone variability. The results show that the peak phase of ENSO significantly impacts the interannual variability of Antarctic spring (September-October) stratospheric ozone in decaying years. Specifically, during the decaying year of El Niño (or La Niña), lower stratospheric ozone depletion is reduced (or enhanced) in Antarctic springtime. During the peak phase of El Niño, tropical SSTA intensifies convection and weakens upper tropospheric winds over the central and eastern equatorial Pacific, allowing more wave momentum fluxes from the troposphere into the stratosphere. In the decaying years, anomalous wave trains in both the troposphere and stratosphere link the tropical lower-atmospheric dynamics with the mid-high latitude stratospheric dynamics. Moreover, in the Southern Hemisphere under El Niño, the enhanced upward propagation of planetary waves accelerates the Brewer-Dobson circulation (BDC) and decelerates the mid-latitudes stratospheric zonal wind. Concurrently, polar stratospheric warming destabilizes the polar vortex in the decaying year, suppressing Antarctic springtime ozone depletion. In contrast, following La Niña, these coupling mechanisms

typically reverse, leading to mid-latitude stratospheric zonal wind acceleration and polar stratospheric cooling, which strengthen the polar vortex and thus enhance ozone depletion. These findings advance understanding of ENSO-ozone teleconnections and inform ozone recovery predictions.

Keywords: ENSO; Brewer-Dobson circulation; Ozone recovery; Antarctic

1. Introduction

The interannual variability of the Antarctic ozone hole is influenced by various coupled processes influencing stratospheric chemistry and dynamics (Newman, 2010; Tung et al., 1986). Antarctic ozone fluctuations not only affect the local stratospheric environment but also exert a profound influence on the Southern Hemisphere (SH) climate via atmospheric circulation (Fogt and Marshall, 2020; Polvani et al., 2011; Yook et al., 2022). During Antarctic winter-spring, persistent cold stratospheric temperatures and a stabilized vortex facilitate the formation of polar stratospheric clouds (PSCs), sustaining seasonal ozone depletion (Newman, 2010; Solomon, 1999). Since the implementation of the Montreal Protocol and the regulation of ozone-depleting substances (ODSs), the Antarctic ozone layer is displaying a recovering trend in spring (Chipperfield et al., 2017; Kuttippurath and Nair, 2017; Solomon et al., 2016). Under relatively stabilized ODS concentrations, dynamical processes, such as the Brewer-Dobson circulation (BDC), planetary wave propagation, sudden stratospheric warmings (SSWs), and Quasi-Biennial Oscillation (QBO), gradually dominate ozone hole variability (Kessenich et al., 2023; Orr et al., 2012), mainly by perturbing polar vortex stability and photochemistry. El Niño-Southern Oscillation (ENSO) is another key factor affecting stratospheric ozone, with well-documented impacts on the long-term ozone variability (Jeong et al., 2023; Li et al., 2023; Lin and Qian, 2019; Xie et al., 2014).

As the leading mode of the global interannual climate variability, ENSO triggers a series of large-scale wave trains through atmospheric thermal and dynamical processes, significantly influencing extreme events such as precipitation, drought, and tropical cyclones, with impacts extending to the stratosphere via planetary wave upward propagation (Chang et al., 2024; Domeisen et al., 2019; Eichler and Higgins, 2006; Sheng et al., 2025). The influence of ENSO on tropical troposphere-stratosphere interactions has been widely reported (Benito-Barca et al., 2022; Calvo et al., 2008; Wang et al., 2011). For example, in the tropical troposphere, ENSO directly alters tropical ozone distribution, while at mid-high latitude stratosphere, it modulates ozone by altering planetary wave propagation and the strength of the BDC (Garfinkel et al., 2018; Oman et al., 2013; Zhang et al., 2015). In the Arctic, El Niño-related stratospheric warming and polar vortex weakening have been identified. The stratospheric signals of ENSO and QBO represent a linear superposition, with different phase combinations producing distinct polar vortex responses (Garfinkel and Hartmann, 2008; Wang et al., 2024a; Wang et al., 2024b). ENSO has also been found to impact stratospheric ozone differently across hemispheres (Li et al., 2023), yet its specific influence on Antarctic stratospheric ozone remains less understood.

For the Antarctic, the ENSO teleconnection disturbs temperature at mid-high latitude stratosphere in the SH and has a significant impact on the ozone in the polar region by modulating the stratospheric circulation (Domeisen et al., 2019; Sigmond et al., 2011), with previous studies highlighting event-dependent responses. For instance, Yang et al. (2015) discovered that neutral and Central Pacific (CP) El Niño events show distinct impacts on Antarctic stratospheric temperature and planetary waves, while Rao and Ren (2020) found that warming SSTA in the tropical Pacific favours the southward displacement of the winter polar vortex and the eastward movement of the southern circumpolar westerly jet. This indicates that ENSO is closely related to the variations of planetary waves and the SH stratosphere, and the wave flux accumulated in the SH autumn-spring causes lead-lag responses. More recently, Niu et al. (2023) found that sea surface temperature anomalies (SSTA) caused by the ENSO Modoki in September-October drive Antarctic stratospheric ozone anomalies in October-November. However, the broader lagged impacts of unclassified ENSO events on Antarctic ozone have not been clearly explained. This study focuses on the lagged effects of ENSO on the interannual variability of Antarctic spring ozone.

Although ozone recovery has been evident across various latitudes since 2000, the Antarctic ozone hole remains a major concern, requiring ongoing monitoring to ensure sustained overall recovery (Chehade et al., 2014; Kuttippurath et al., 2013; Weber et al., 2022). In particular, springtime recovery is sensitive to stratospheric ozone changes. Kessenich et al. (2023) found that ozone reduction dominated the stratosphere in October since 2004, emphasizing the role of dynamic processes. The mechanism pathways between dynamic processes such as stratospheric circulation anomalies caused by ENSO and the ozone depletion in the Antarctic spring require further understanding. Stone et al. (2022) identified a stratospheric pathway that links ENSO to SH circulation during austral summer. Through diagnostic examination of tropical convection anomalies, vertical propagation of planetary waves, and stratospheric dynamic processes, this study quantifies the 9-12 month lagged effect of ENSO and proposes an ENSO teleconnection pathway through which ENSO events modulate Antarctic spring stratospheric ozone.

This study is organized as follows: Section 2 presents datasets and analysis methodologies. Section 3 analyzes the relationship between ENSO and Antarctic spring stratospheric ozone. Section 4 describes the mechanism behind the lagged effect of ENSO on Antarctic springtime ozone through stratosphere-troposphere dynamical and chemical processes. Section 5 summarizes the major conclusions.

2. Data and methods

2.1. Data

Ozone profile datasets used here comprise the Microwave Limb Sounder (MLS), Stratospheric Water and Ozone Satellite Homogenized (SWOOSH), Modern-Era Retrospective Analysis for Research and Applications, version 2 (MERRA2) from satellite observation and reanalysis, as well as the global three-dimensional chemical-transport (TOMCAT/SLIMCAT 3-D chemical transport model) and chemistry-climate (Whole Atmosphere Community Climate Model) model.

The MLS onboard the NASA Aura satellite has been providing global data on composition, temperature, and humidity from the upper troposphere to the mesosphere since August 2004. MLS offers good coverage of ozone distribution and profiles (Dhomse et al., 2022; Livesey et al., 2008).

The SWOOSH ozone dataset from 1984 to present is processed from limb sounding and solar occultation satellites (Davis et al., 2016). Processing yields monthly means, variances, and uncertainty estimates for individual sources and merged datasets. The SWOOSH dataset, with its monthly resolution, is well-suited for analyzing long-term ozone changes, trends, and seasonal variations in the troposphere-stratosphere (Li et al., 2023; Szeląg et al., 2020; Zhang et al., 2021). Its data are used primarily to analyze the zonal distribution of ozone. The data are available at https://csl.noaa.gov/groups/csl8/swoosh.

The Whole Atmosphere Community Climate Model, version 6 (WACCM6), developed by the National Center for Atmospheric Research, is a global climate model. WACCM6 can well reproduce the dynamical and chemical processes between the troposphere and stratosphere and provides a basis for daily forecasts (Davis et al., 2023; Gettelman et al., 2019). It extends from the Earth's surface to about 140 km in altitude, enabling comprehensive analysis of ozone profiles and distribution.

TOMCAT/SLIMCAT 3-D chemical transport model (TOMCAT) is a global chemical transport model (CTM) containing a detailed stratospheric chemistry scheme (Chipperfield, 2006). TOMCAT CTM is forced with ERA5 reanalysis data, ensuring state-of-the-art past meteorological information is used for consistency to simulate ozone transport driven by the BDC, QBO, and planetary wave perturbations. The model setup is similar to the one used in Zhou, X. et al. (2024). Briefly, the model uses time-varying lower boundary conditions for ODSs and greenhouse gases (GHGs) from WMO (2022). It also includes time-varying solar fluxes and stratospheric sulphate aerosol area density (SAD) until 2024 as described in Dhomse et al. (2016); Dhomse et al. (2015). TOMCAT, as a global model, can simulate long-term ozone change and spatial distribution with good results. Table 1 compares the ozone datasets.

Zonal wind, temperature, and geopotential height data with horizontal resolution of 0.25° × 0.25° and 37 vertical levels were obtained from the ERA5 reanalysis dataset. Outgoing Longwave Radiation (OLR) data were obtained from the Top net thermal radiation in the ERA5 reanalysis dataset. Sea surface temperature (SST) data are from the Hadley Centre Sea Ice and Sea Surface Temperature dataset (HadISST), developed by the Hadley Centre for Climate Change at the UK Met Office. The Oceanic Niño Index (ONI) from the National Weather Service Climate Prediction Center. It represents the 3-month running mean of ERSST.v5 sea surface temperature anomalies in the Niño 3.4 region (5°N-5°S, 120°-170°W). The data can be accessed (http://origin.cpc.ncep.noaa.gov/products/analysis_monitoring/ensostuff/ONI_v5.php).

Table 1

Ozone dataset.

Dataset	Start and end year	Temporal resolution	Spatial resolution
TOMCAT	1979-2024	Monthly	Horizontal resolution of 2.8° × 2.8° and 32 vertical levels (about 0-60km)
MERRA2	1980-2024	Monthly	Horizontal resolution of 0.5° × 0.625° and 42 vertical levels (1000-0.1hPa)
MLS	2004-2024	Monthly	Horizontal resolution of 2.8° zonal mean with 37 vertical levels(1000-0.1hPa)
WACCM6	1980-2014	Monthly	Horizontal resolution of 1.875° × 2.5° and 88 vertical levels (about 0-140km)
SWOOSH	1984-2024	Monthly	Horizontal resolution of 5° × 20° and 31 vertical levels (316hPa-1hPa)

2.2. Methods

Following the National Oceanic and Atmospheric Administration's (NOAA) ONI classification protocol, this analysis uses ONI to delineate the ENSO from 1979 to 2023 (Bamston et al., 1997). An event is defined as El Niño (La Nina) when ONI is ≥0.5°C (≤-0.5°C) for at least five consecutive months (Fig. 1). ENSO also includes single-year and multi-year events. Multi-year events, persisting for two or more years (e.g., September 2014–April 2016 El Niño), tend to produce cumulative effects. To isolate the lagged effects of ENSO events, multi-year events are excluded in this study. Observational results combined with the recharge oscillation theory and delayed oscillator theory show that the peak phase of ENSO occurs around the Northern Hemisphere (NH) winter. The decay phase of ENSO occurs around the SH autumn, and its occurrence year is defined as the decaying year. According to Fig. 2b, the decaying year of ENSO is identified as the primary impact year. The occurrence and impact of ENSO years are summarized in Table 2.

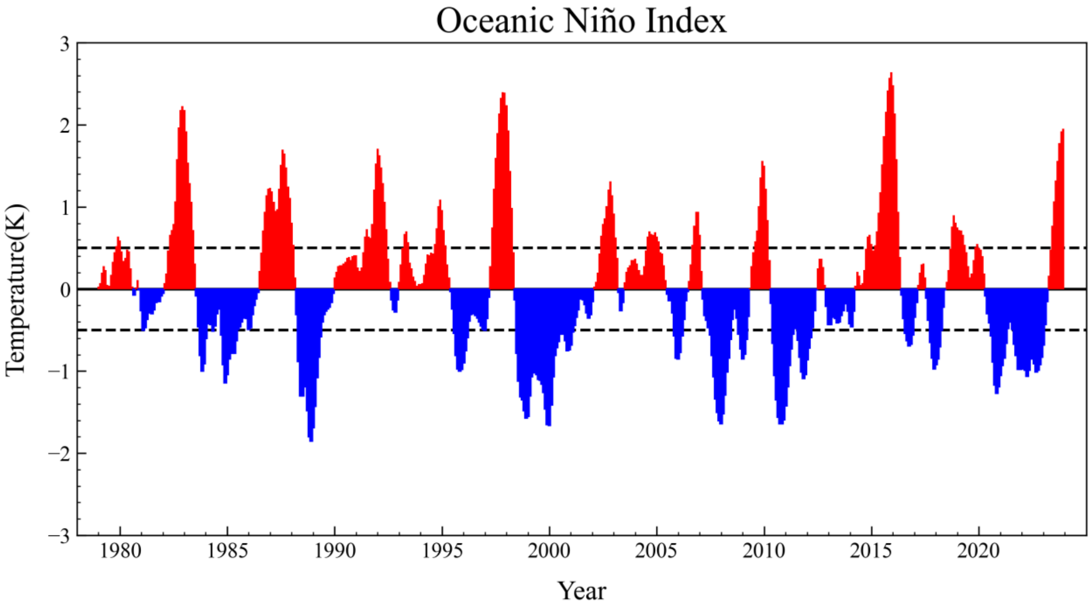

Fig. 1. The Oceanic Niño Index (ONI) time series from 1979 to 2023.

Table 2
Years of ENSO occurrence and impact.

Event	Occurrence years	Impact year
El Niño	1982-1983, 1991-1992, 1994-1995, 1997-1998, 2002-2003, 2004-2005, 2009-2010, 2018-2019	1983, 1992, 1995, 1998, 2003, 2005, 2010, 2019
La Niña	1983-1984, 1984-1985, 1988-1989, 1995-1996, 2005-2006, 2007-2008, 2008-2009, 2010-2011, 2011-2012, 2017-2018, 2020-2021	1984, 1985, 1989, 1996, 2006, 2008, 2009, 2011, 2012, 2018, 2021

To characterize wave propagation, we use the Eliassen-Palm (E-P) flux, which is an approximate proxy for the strength of the upward-propagating waves that drive the stratospheric circulation. The zonal (F_y) and vertical (F_z) components of the E-P flux, as well as the E-P flux divergence (D_F), are calculated using the method for quasi-geostrophic 2-D E-P flux (Andrews et al., 1987). The formulae are as follows:

$$F_y = -\rho_0 \alpha \cos\varphi \, \overline{u'v'}$$

$$F_z = -\rho_0 \alpha \cos\varphi \frac{Rf}{HN^2} \overline{v'T'}$$

$$D_F = \frac{\nabla \cdot F}{\rho_0 \alpha \cos\varphi} = \frac{\partial(F_y \cos\varphi)/\alpha \cos\varphi \, \partial\varphi + \partial F_z/\partial z}{\rho_0 \alpha \cos\varphi} \quad (1)$$

where ρ_0 is air density; α is Earth's radius; φ is latitude; u and v are the zonal and meridional components of the wind; R is the gas constant; f is the Coriolis parameter;

H is atmospheric altitude (km); T is temperature. The overline indicates the zonal mean, and the prime indicates deviation from the zonal mean.

3. Response between Antarctic ozone and ENSO

The core area of ozone depletion in the Antarctic ozone hole lies in the lower stratosphere, so this study investigates long-term variations in Antarctic spring stratospheric ozone using multiple observational datasets (60°S–90°S; 10–100 hPa; September–October mean). Fig. 2a shows the long-term time series of Antarctic stratospheric partial column ozone (PCO) from 1979 to 2023. PCO declined steadily until around 2000, when international regulations on halogenated ozone-depleting substances halted the trend. Despite this stabilization, PCO continues to fluctuate significantly between 90 and 150 Dobson Units (DU), with consistent interannual variability across multiple datasets of different temporal coverage. Notably, the time series also captures distinct ozone anomalies caused by exceptional stratospheric events, such as the SSWs in 2002 and 2019. Previous studies attribute the 2019 SSW to factors such as the equatorial QBO and the central Pacific SSTA (Rao et al., 2020).

Fig. 2b illustrates the lag correlation between Antarctic spring stratospheric ozone and ONI. To reduce limitations in data coverage and continuity, lag correlation analysis was performed using the TOMCAT dataset, which offers an extensive temporal span, global coverage, high spatial resolution, and robust continuity. Analysis reveals a statistically significant correlation, with the ENSO leading Antarctic stratospheric ozone by 9-12 months. Phase relationships demonstrate that the peak phase of ENSO influences Antarctic spring ozone anomalies in the decaying year.

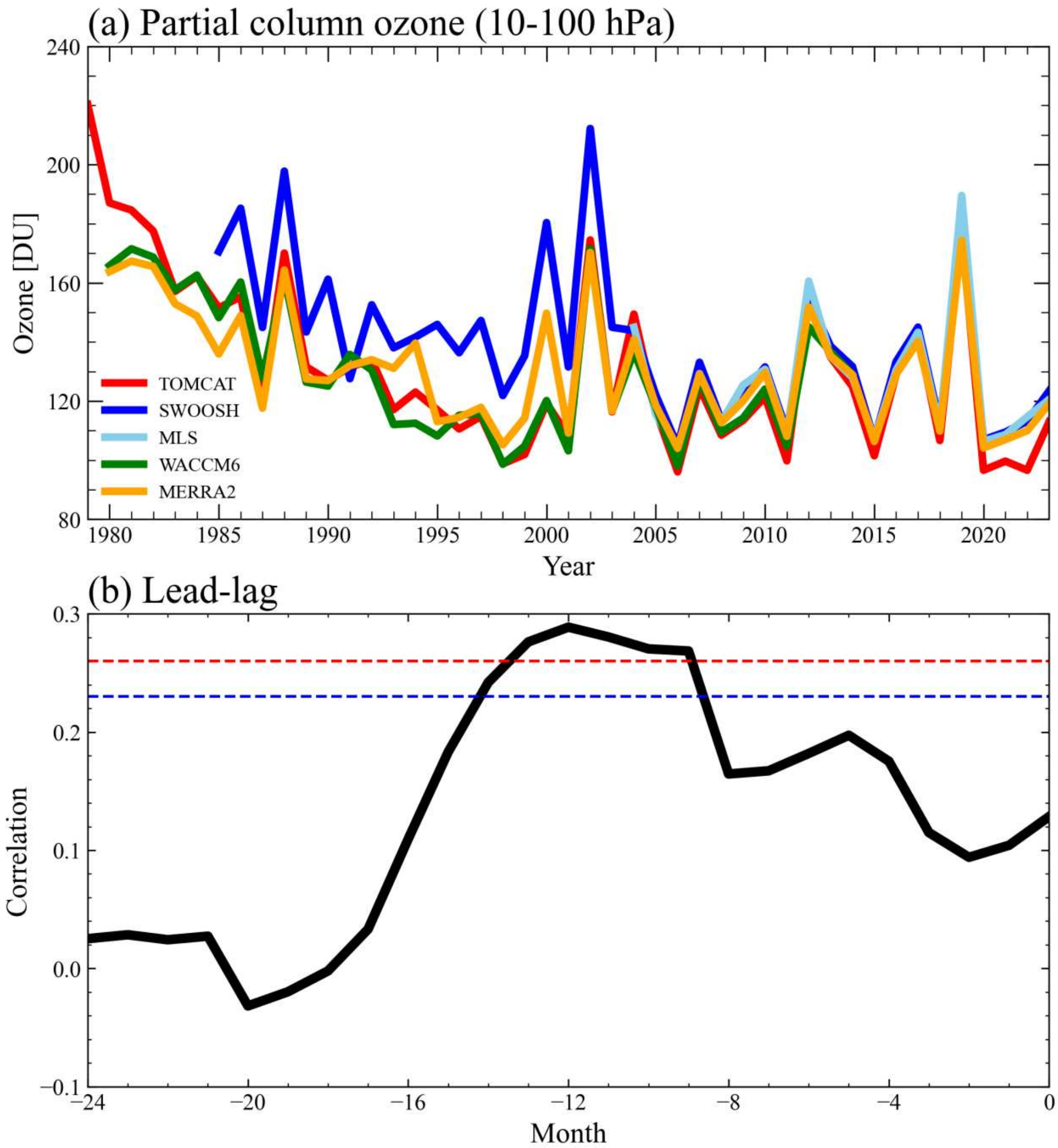

Fig. 2. Antarctic spring stratospheric ozone variability (1979-2023): (a) Multi-dataset comparison of partial column ozone (10-100 hPa, September-October mean); (b) Lag correlation between TOMCAT ozone and ONI. Red dashed line: 90% t-test, blue dashed line: 85% t-test.

Fig. 3 shows the ozone difference between ENSO composite events (El Niño composite minus La Niña composite, El-La), revealing a significant positive ozone anomaly in the 20-50 hPa layer of the Antarctic spring stratosphere. This indicates that ozone concentrations during the decaying year of El Niño are significantly higher than those following La Niña events. In contrast, the tropical stratosphere exhibits predominantly negative ozone anomalies. The results are consistent across multiple datasets.

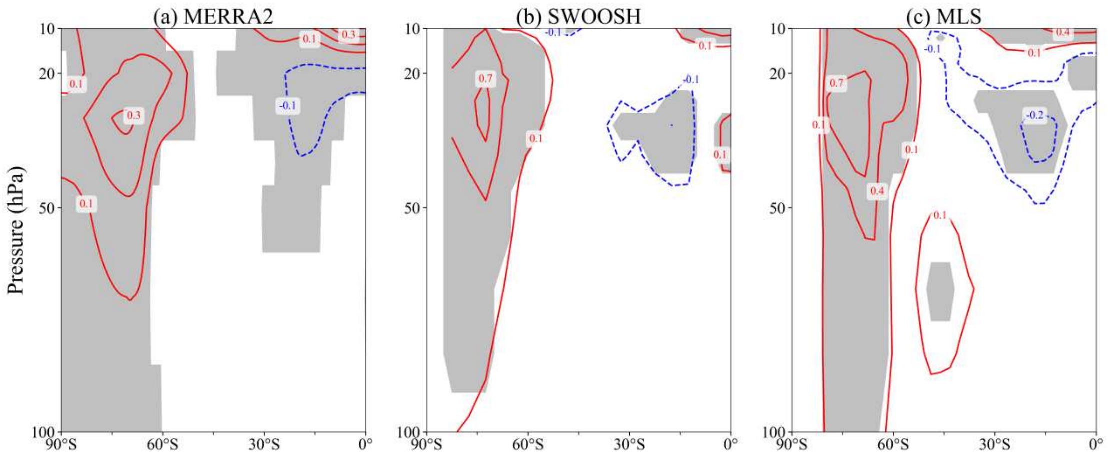

Fig. 3. Composite differences of zonal mean ozone (unit: ppmv) in the decaying year (September–October mean in the SH spring) between El Niño and La Niña years (El-La) for different datasets: (a) MERRA2, (b) SWOOSH, (c) MLS. Significant anomalies above the 90% confidence level according to the Monte Carlo test are indicated by the grey areas.

Fig. 4 presents zonal mean temperature anomalies during the peak phases of ENSO (December–March) based on the ERA5 dataset, with the grey areas indicating statistical significance. During the peak phase of ENSO, El Niño events are associated with positive temperature anomalies in the equatorial troposphere, resulting in significantly higher mean temperatures than La Niña. This anomaly can persist until March and extends from the tropical troposphere to the mid-latitude lower stratosphere, with a positive temperature anomaly reaching 1 K. Such significant temperature anomalies further affect the stratospheric residual circulation through abnormal tropical convection and planetary wave propagation.

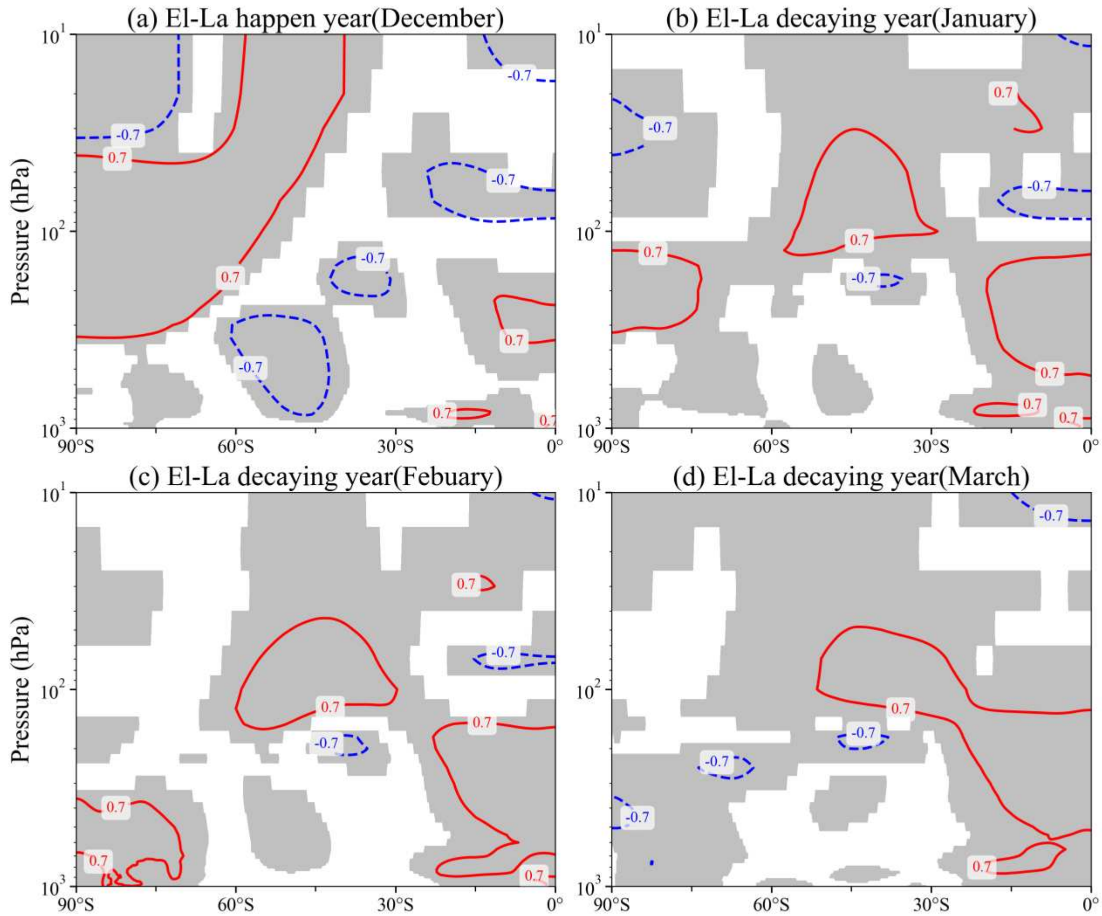

Fig. 4. Composite differences in zonal mean temperatures (unit: K) for El-La. (a) December, (b) January, (c) February, (d) March. Significant anomalies above the 90% confidence level according to the Monte Carlo test are indicated by the grey areas.

Convective activity is an important source of thermal structure and zonal wind changes in the upper atmosphere. Fig. 5 shows OLR from the peak to the decay period of El-La, with significant anomalies in the equatorial region. The OLR shows a negative pattern in the central and eastern equatorial Pacific, which also indicates enhanced convective activity above during El Niño events than during La Niña events.

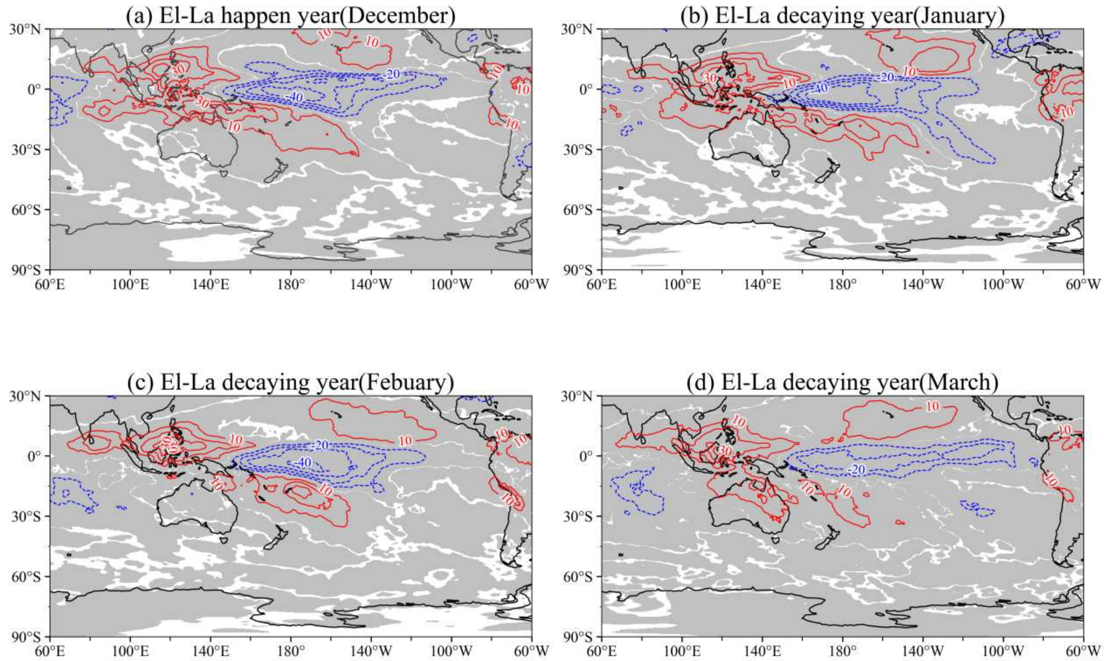

Fig. 5. Composite differences in OLR (unit: J m^{-2}) for El-La. (a) December, (b) January, (c) February, (d) March. Significant anomalies above the 90% confidence level according to the Monte Carlo test are indicated by the grey areas.

The equatorial zonal wind is often defined as the average zonal wind between 5°S and 5°N (Zhou, T. et al., 2024). Fig. 6 shows the differences in this quantity during ENSO composite events to reveal the impact of tropical SSTA on stratospheric dynamics processes. In the upper troposphere, westerly winds during El Niño are weaker than during La Niña over the central and eastern equatorial Pacific. The difference in zonal wind from December to the following March shows that the Walker circulation during El Niño events is weaker than during La Niña events over the equatorial Pacific (140°E -100°W). The weakening of the Walker circulation during El Niño periods has also been confirmed. The weaker upper tropospheric winds during the El Niño period mean that more wave momentum flux is transmitted to the stratosphere (Kawatani et al., 2019).

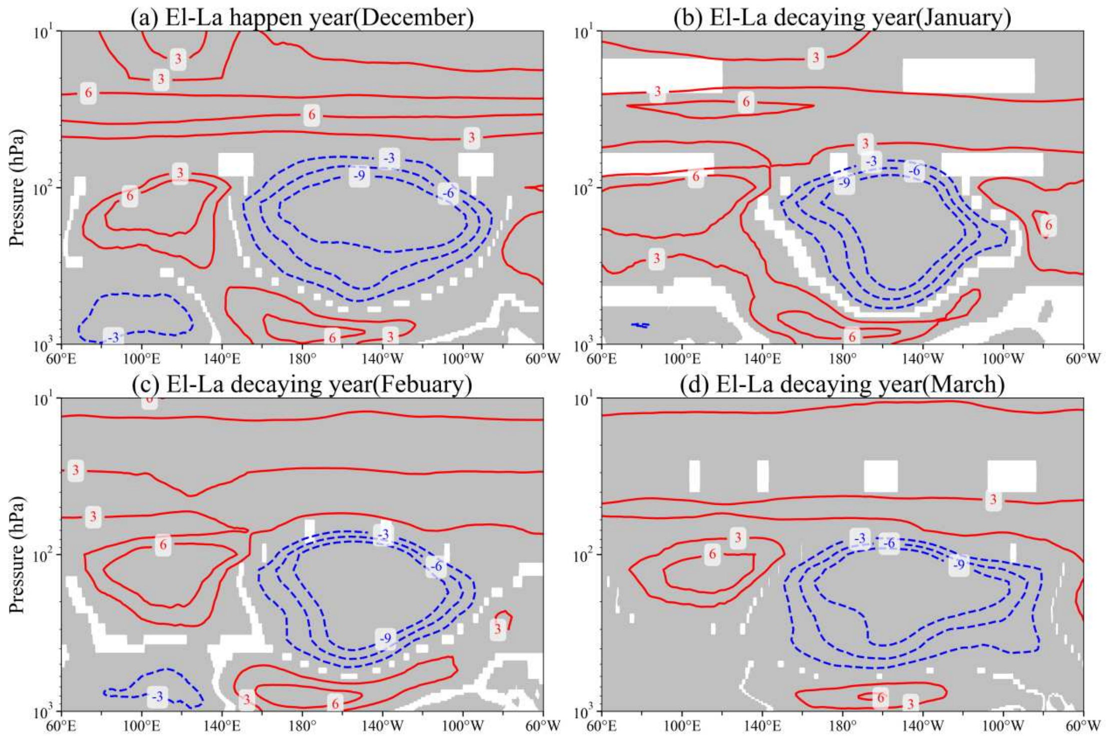

Fig. 6. Composite differences in zonal wind (unit: m s^{-1}) for El-La in the equatorial region (5°S-5°N) for (a) December, (b) January, (c) February, and (d) March. Significant anomalies above the 90% confidence level according to the Monte Carlo test are indicated by the grey areas.

A weakened (enhanced) Walker circulation leads to a shortened (lengthened) QBO period during El Niño (La Niña). Zonal wind anomalies persist into the decay phase of ENSO, indicating that the sustained SSTA significantly impacts the troposphere and the stratosphere. Fig. 7 shows the geopotential height anomalies at 200 hPa during the decay phases of ENSO (April–July), revealing wave propagation pathways from tropical to mid-high latitudes. April–July composite maps show alternating positive and negative centres of geopotential height anomaly over the South Pacific, forming a wave train that extends from the subtropical Pacific to the polar region. The gradual southward shift of the negative geopotential height anomaly centres indicates enhanced planetary wave anomalies propagation from the tropics to mid-high latitudes through the troposphere. During El Niño, the geopotential wave train is statistically significant, with more planetary waves propagating to the mid-high latitude stratosphere of the SH.

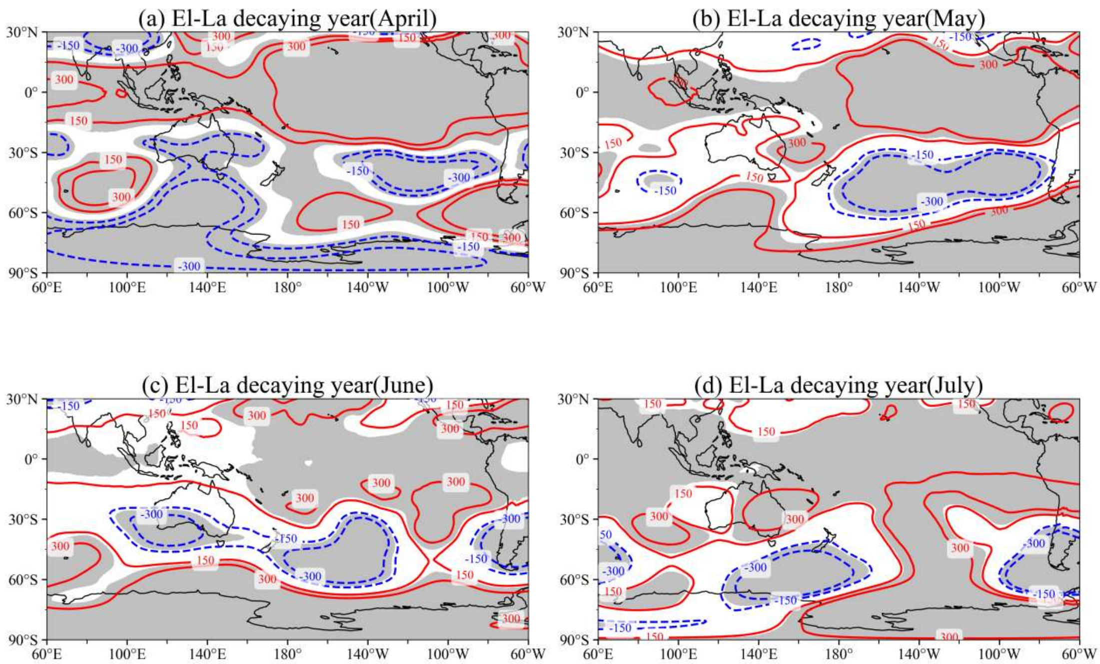

Fig. 7. Composite differences in geopotential heights (unit: $m^2 s^{-2}$) at 200 hPa for El-La in the decaying year. (a) April, (b) May, (c) June, and (d) July. Significant anomalies above the 90% confidence level according to the Monte Carlo test are indicated by the grey areas.

Considering the persistent impact of upward wave propagation on the polar region during the SH autumn-winter, this study analyzes the responses of zonal mean temperature and zonal wind anomalies to the SSTA during ENSO composite events from July to September. Figs. 8a-c show positive stratospheric anomalies in SH mid-high latitudes during spring and winter, reaching 3.5 K in July and intensifying to 7.5 K over the polar region by September. Figs. 8d-e reveal a clear negative zonal wind anomaly in the mid-latitude stratosphere, with a deceleration of up to 5 m/s. Combined with the thermal wind balance, the negative anomalous zonal wind in the mid-latitude stratosphere corresponds to the positive anomalous temperature at high latitudes. Collectively, in the SH spring-winter, temperature anomalies move towards the poles along with zonal wind anomalies.

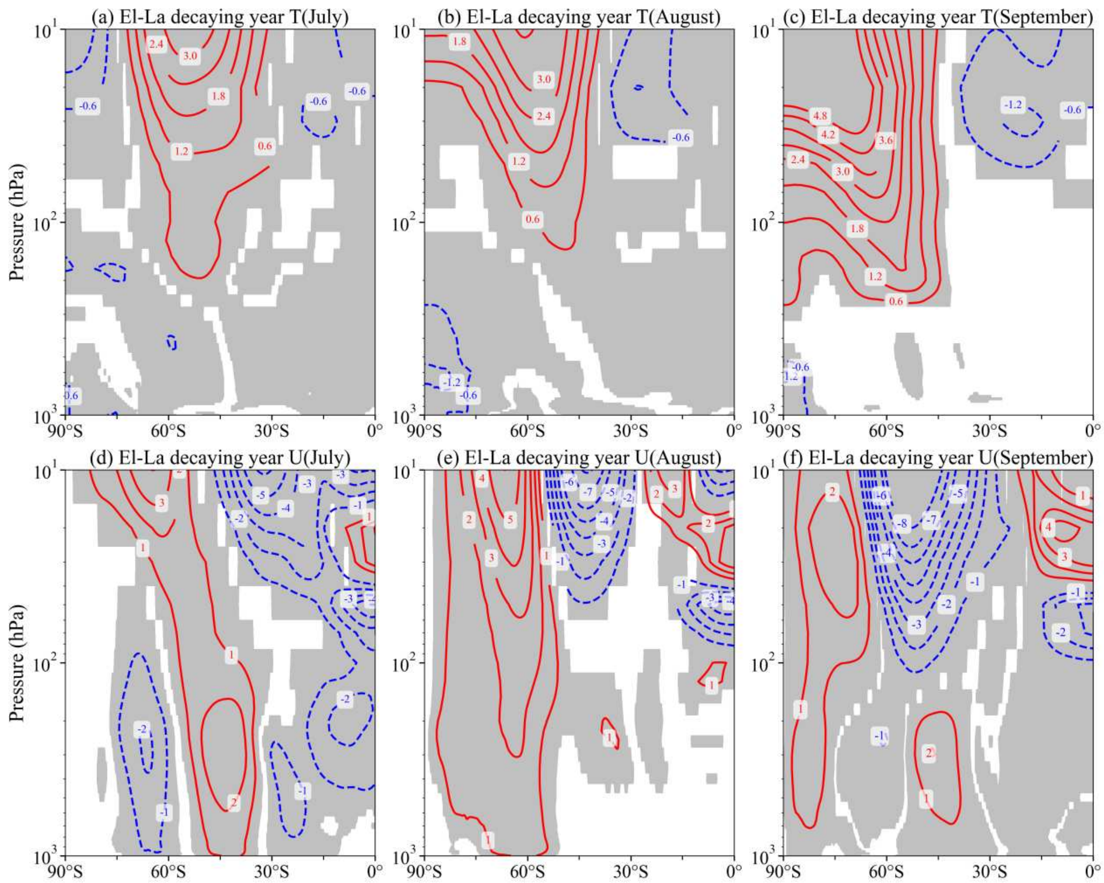

Fig. 8. Composite differences in (a-c) zonal mean temperature (unit: K) and (d-e) zonal winds (unit: m s^{-1}) for El-La in the decaying year. (a) and (d) July, (b) and (e) August, (c) and (f) September. Significant anomalies above the 90% confidence level according to the Monte Carlo test are indicated by the grey areas.

4. Discussion

4.1 Planetary Wave Activity

ENSO-forced planetary wave propagation anomalies modulate stratospheric circulation, and ozone redistribution is controlled by meridional circulation changes and planetary wave dissipation. Yang et al. (2015) reported intensified planetary wave activity in the SH stratosphere from July to September during most CP El Niño years. Fig. 9 demonstrates the composite anomalies of E-P flux divergence based on ERA5 datasets, revealing intensified vertical planetary wave propagation in SH mid-high latitudes under El Niño. Enhanced wave dissipation perturbs stratospheric westerlies through momentum flux convergence anomalies, inducing mid-latitude zonal wind deceleration (Fig. 8d–f) and BDC intensification.

Previous studies have shown that Central Pacific (CP) El Niño events increase stratospheric temperatures in the SH during spring and winter, weakening the polar vortex and enhancing the BDC (Hurwitz et al., 2011; Xie et al., 2012; Yang et al., 2015). More planetary waves are transmitted into the stratosphere, increasing polar temperatures (Fig. 8a-c). Such temperature anomalies play an important role in stratospheric ozone, as anomalous temperatures during El Niño weakened the polar vortex stability and decreased ozone depletion (Fig. 3).

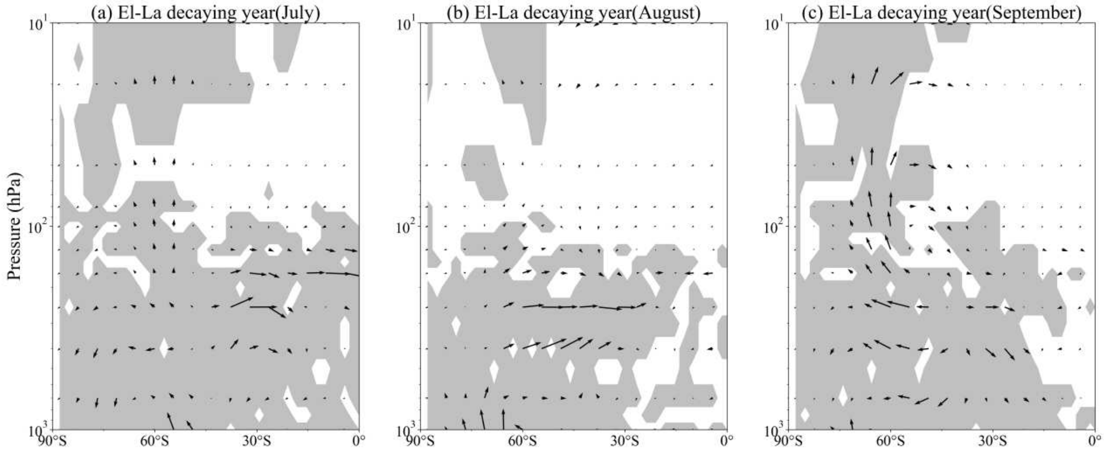

Fig. 9. Composite differences in E-P fluxes (vectors) and E-P flux divergence (contours) for El-La in the decaying year. (a) July, (b) August, and (c) September. Significant anomalies above the 90% confidence level according to the Monte Carlo test are indicated by the grey areas.

Studies show that ENSO modulates stratospheric ozone mainly through (1) planetary wave upward propagation efficiency and (2) BDC strength, quantified by the cumulative eddy heat flux (EHF) at 100hPa in spring (Newman et al., 2001; Weber et al., 2011). In the SH from March to September, the wave flux accumulated at mid-high latitudes propagates upward to the stratosphere, affecting the BDC and the stratospheric polar vortex. As shown in Table 3, the EHF of El Niño begins higher than that of La Niña in the SH autumn, and the difference gradually increases and peaks in spring. These results indicate stronger planetary wave activity in the SH stratosphere during the decaying years of El Niño compared to La Niña, consistent with Domeisen et al. (2019), who suggested El Niño significantly modulates planetary wave activity and its interaction with the stratospheric polar vortex.

Table 3
Mean Eddy Heat Flux (45°–75°S) at 100 hPa: The Years of ENSO in March-May, June-August, and September-October.

	El Niño	La Niña
March-May	-6.28	-6.09
June-August	-8.76	-7.60
September-October	-15.66	-13.42

4.2 Chemical-dynamical coupling

The mechanism of ENSO teleconnection on Antarctic stratospheric ozone is closely related to the chemical and dynamical processes of the coupled stratosphere-troposphere system caused by SSTA. From July to September, a positive temperature anomaly was observed in the mid-high latitude stratosphere. PSCs were present from June to September, associated with cold temperatures below 195 K (Solomon, 1999). Fig. 10 shows the daily average temperature of Antarctica (60°S–90°S, 100 hPa) from July to September in the decaying year. During El Niño events (Fig. 10a), temperatures typically drop below the PSC threshold (195 K) by late July but rise above it by September. On the contrary, during most La Niña events, temperatures remain below the threshold for a longer period (Fig. 10b). The PSCs area expands throughout early winter, and its variations are closely linked to the duration of low average temperatures (Roy et al., 2024). During El Niño, higher temperatures and shorter cold periods lead to a reduced PSC area, thereby decreasing ClO-catalyzed ozone depletion.

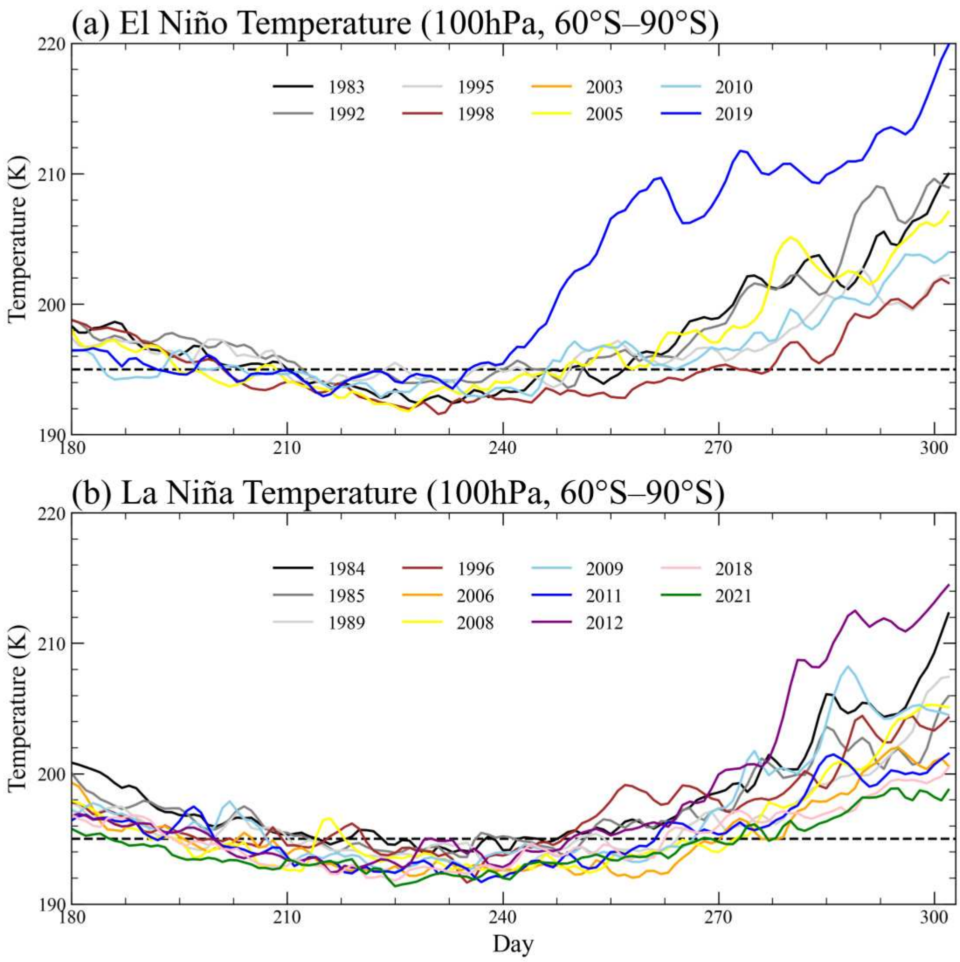

Fig. 10. The daily average temperature (unit: K) of Antarctica (60°S–90°S) from July to October in the decaying year at 100hpa. (a) El Niño, (b) La Niña. The black dotted line represents 195 K.

4.3 Teleconnection pathways

The ENSO teleconnection mechanism directly links ENSO-forced tropospheric anomalies to springtime polar ozone variability via a stratospheric dynamics transport pathway. Combined SSTA and OLR anomalies suggest that warming (cooling) of the tropical sea surface leads to weakening (strengthening) of the westerly winds during El Niño (La Niña), affecting the Walker circulation. A weakened Walker circulation leads to a shortened QBO period during El Niño. Wang et al. (2022) found that the QBO impacts on ozone are mainly through dynamic transport and related to temperature-dependent chemical processes. Yamashita et al. (2018) further identified enhanced upward planetary wave in the lower stratosphere during the westerly QBO as a key pathway connecting the QBO with the SH stratospheric polar vortex. These findings indicate that ENSO influences dynamic processes such as the BDC through upward wave propagation, thus regulating the transport efficiency of stratospheric ozone and polar vortex stability (Garfinkel and Hartmann, 2008; Lim et al., 2018).

The equatorial SSTA perturbation stimulates convective activities, altering upper atmosphere temperatures and tropical zonal winds. Decelerated (accelerated) tropical zonal winds facilitate increased (reduced) upward transmission of wave momentum flux into the stratosphere (Fig. 6). Evtushevsky et al. (2019) reported interacting tropospheric and stratospheric pathways of the teleconnection to strongly enhance the central tropical Pacific impact. The teleconnection mechanism between ENSO and the SH stratosphere still needs to be clarified. Stone et al. (2022) found that the stratospheric circulation acts as an intermediary linking ENSO to tropospheric variability during SH spring and summer. Based on this, a novel teleconnection pathway by which ENSO influences Antarctic ozone variability with a lag of 9–12 months is proposed (Fig. 11).

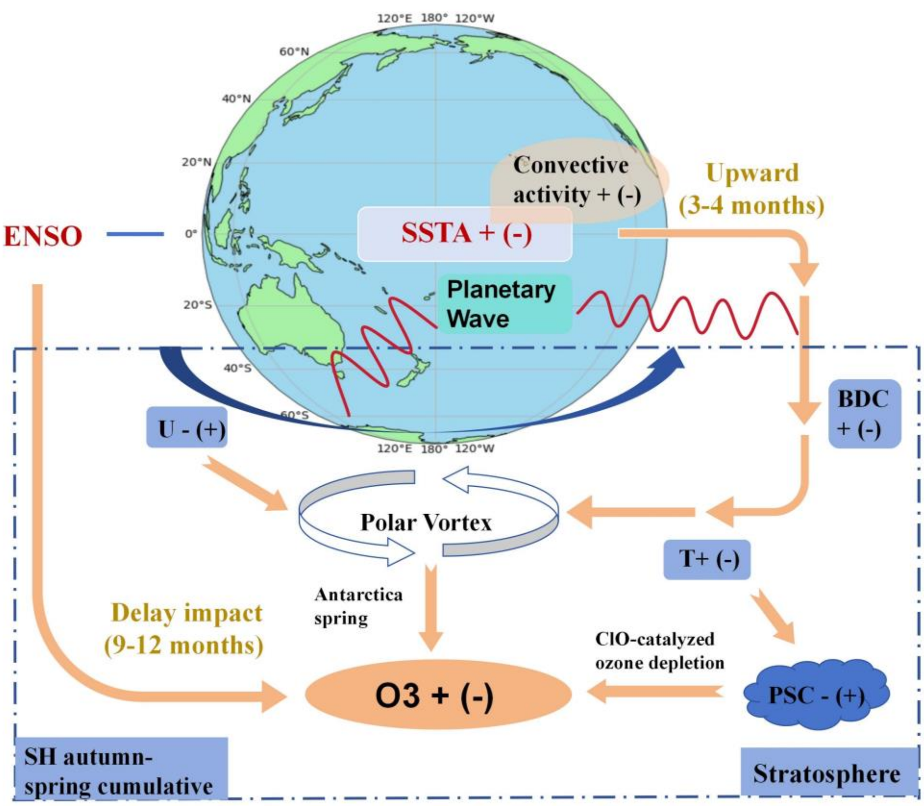

Fig. 11. Lagged ENSO teleconnection pathways driving Antarctic ozone variability (time lag: 9-12 months).

Fig. 11 summarizes the stratosphere-troposphere pathways through which ENSO modulates Antarctic spring ozone interannual variability. Dynamically, ENSO-forced planetary wave propagation anomalies modulate stratospheric circulation and stratospheric zonal wind anomalies in the mid-latitudes. BDC strengthens (weakens), directly enhances (suppresses) meridional ozone transport from the tropics. Zonal winds and BDC anomalies in the mid-high latitude stratosphere further modulate stratospheric temperature and polar vortex stability, thus influencing the PSCs area and stratospheric ozone depletion. The peak phase of ENSO significantly impacts Antarctic spring stratospheric ozone through cross-seasonal and interhemispheric dynamical pathways.

5. Conclusions

This study integrates satellite-based observations, reanalysis datasets, as well as 3-D chemical-transport and chemistry-climate model simulations to explore the impact of ENSO on Antarctic spring stratospheric ozone and analyzes the teleconnection mechanisms of the tropical SSTA effect on Antarctic ozone. Analysis reveals ENSO exerts a 9-12 month lagged influence on Antarctic spring stratospheric ozone during its decaying year, reducing ozone depletion following El Niño and enhancing it following La Niña. This result agrees with previous findings that ozone anomalies over Antarctica occur one year after ENSO (Lin and Qian, 2019).

Our study proposes a novel stratosphere-troposphere teleconnection pathway between ENSO and Antarctica spring ozone interannual variability. ENSO, represented by tropical SSTA, affects upward propagation of planetary waves and associated stratospheric dynamics in the SH, thereby modulating the spring polar ozone depletion during the decaying year. In particular, El Niño (La Niña) events strengthen (weaken) the BDC and decrease (increase) zonal winds at middle latitudes, affecting the polar temperatures and ozone depletion. This mechanism advances the mechanistic understanding of ENSO teleconnections in the SH stratosphere.

In addition, the stratospheric pathway proposed has significant implications for the Southern Hemisphere circulation and regional climate. These findings provide critical dynamic factor references for ozone recovery prediction. Nevertheless, the influence and mechanisms of different ENSO types (e.g., Eastern Pacific vs. Central Pacific El Niño) and multi-year events (e.g., the 2014–2016 El Niño) affecting Antarctic ozone warrant further investigation.

CRediT authorship contribution statement

Haotian He: Writing – review & editing, Writing – original draft, Data curation, Methodology, Visualization, Investigation, Formal analysis. Shujie Chang: Writing – review & editing, Writing – original draft, Conceptualization, Methodology, Funding acquisition. Wuhu Feng: Writing – review & editing, Methodology, Supervision. Martyn P. Chipperfield: Writing – review & editing, Resources, Data curation,

Supervision. Sandip S. Dhomse: Writing – review & editing. Yuwen Li: Writing – review & editing, Visualization. Saffron Heddell: Writing – review & editing.

Declaration of competing interest

The authors declare that they have no known competing financial interests or personal relationships that could have appeared to influence the work reported in this paper.

Acknowledgments

This study was supported by National Natural Science Foundation of China (42475082), Guangdong Basic and Applied Basic Research Foundation (2023A1515011323), Tropical Ocean Environment in Western Coastal Waters Observation and Research Station of Guangdong Province (2024B1212040008), Innovative Team Plan for Department of Education of Guangdong Province (2023KCXTD015), First-Class Discipline Plan of Guangdong Province (080503032101 and 231420003), Innovation Team Project of General University in Guangdong Province of China (2024KCXTD042) and China Scholarship Council (202208440223).

Data availability

Data will be made available on request. The SWOOSH data are available at https://csl.noaa.gov/groups/csl8/swoosh. The ERA5 data are available at https://cds.climate.copernicus.eu/datasets. The MERRA2 data are available at https://disc.gsfc.nasa.gov/datasets?keywords=MERRA2&page=1.

References

Andrews, D.G., Leovy, C.B., Holton, J.R., 1987. *Middle atmosphere dynamics*. Academic Press.

Bamston, A.G., Chelliah, M., Goldenberg, S.B., 1997. Documentation of a highly ENSO-related SST region in the equatorial Pacific: Research note. Atmos. Ocean. 35, 367-383. https://doi.org/10.1080/07055900.1997.9649597.

Benito-Barca, S., Calvo, N., Abalos, M., 2022. Driving mechanisms for the El Niño–Southern Oscillation impact on stratospheric ozone. Atmos. Chem. Phys. 22, 15729-15745. https://doi.org/10.5194/acp-22-15729-2022.

Calvo, N., García-Herrera, R., Garcia, R.R., 2008. The ENSO signal in the stratosphere. Ann. N. Y. Acad. Sci. 1146, 16-31. https://doi.org/10.1196/annals.1446.008.

Chang, S., He, H., Huang, D., 2024. The effects of gravity waves on ozone over the Tibetan Plateau. Atmos. Res. 299. https://doi.org/10.1016/j.atmosres.2023.107204.

Chehade, W., Weber, M., Burrows, J.P., 2014. Total ozone trends and variability during 1979–2012 from merged data sets of various satellites. Atmos. Chem. Phys. 14, 7059–7074. https://doi.org/10.5194/acp-14-7059-2014.

Chipperfield, M.P., 2006. New version of the TOMCAT/SLIMCAT off-line chemical transport model: Intercomparison of stratospheric tracer experiments. Quarterly Journal of the Royal Meteorological Society: A journal of the atmospheric sciences. 132, 1179–

1203. https://doi.org/10.1256/qj.05.51.

Chipperfield, M.P., Bekki, S., Dhomse, S., Harris, N.R., Hassler, B., Hossaini, R., Steinbrecht, W., Thiéblemont, R., Weber, M., 2017. Detecting recovery of the stratospheric ozone layer. Nature. 549, 211-218. https://doi.org/10.1038/nature23681.

Davis, N.A., Visioni, D., Garcia, R.R., Kinnison, D.E., Marsh, D.R., Mills, M., Richter, J.H., Tilmes, S., Bardeen, C.G., Gettelman, A., 2023. Climate, variability, and climate sensitivity of "middle atmosphere" chemistry configurations of the Community Earth System Model version 2, whole atmosphere community climate model version 6 (CESM2 (WACCM6)). Journal of Advances in Modeling Earth Systems. 15, e2022MS003579. https://doi.org/10.1029/2022MS003579.

Davis, S.M., Rosenlof, K.H., Hassler, B., Hurst, D.F., Read, W.G., Vömel, H., Selkirk, H., Fujiwara, M., Damadeo, R., 2016. The Stratospheric Water and Ozone Satellite Homogenized (SWOOSH) database: a long-term database for climate studies. Earth Syst. Sci. Data. 8, 461-490. https://doi.org/10.5194/essd-8-461-2016.

Dhomse, S.S., Chipperfield, M.P., Damadeo, R.P., Zawodny, J.M., Ball, W.T., Feng, W., Hossaini, R., Mann, G.W., Haigh, J.D., 2016. On the ambiguous nature of the 11 year solar cycle signal in upper stratospheric ozone. Geophys. Res. Lett. 43, 7241-7249. https://doi.org/10.1175/10.1002/2016gl069958.

Dhomse, S.S., Chipperfield, M.P., Feng, W., Hossaini, R., Mann, G.W., Santee, M.L., 2015. Revisiting the hemispheric asymmetry in midlatitude ozone changes following the Mount Pinatubo eruption: A 3-D model study. Geophys Res Lett. 42, 3038-3047. https://doi.org/10.1175/10.1002/2015GL063052.

Dhomse, S.S., Chipperfield, M.P., Feng, W., Hossaini, R., Mann, G.W., Santee, M.L., Weber, M., 2022. A single-peak-structured solar cycle signal in stratospheric ozone based on Microwave Limb Sounder observations and model simulations. Atmos. Chem. Phys. 22, 903-916. https://doi.org/10.5194/acp-22-903-2022.

Domeisen, D.I., Garfinkel, C.I., Butler, A.H., 2019. The teleconnection of El Niño Southern Oscillation to the stratosphere. Rev. Geophys. 57, 5-47. https://doi.org/10.1029/2018RG000596.

Eichler, T., Higgins, W., 2006. Climatology and ENSO-related variability of North American extratropical cyclone activity. J. Clim. 19, 2076-2093. https://doi.org/10.1175/JCLI3725.1.

Evtushevsky, O.M., Grytsai, A.V., Milinevsky, G.P., 2019. Decadal changes in the central tropical Pacific teleconnection to the Southern Hemisphere extratropics. Clim. Dyn. 52, 4027-4055. https://doi.org/10.1007/s00382-018-4354-5.

Fogt, R.L., Marshall, G.J., 2020. The Southern Annular Mode: variability, trends, and climate impacts across the Southern Hemisphere. Wiley Interdiscip. Rev. Clim. Change. 11, e652. https://doi.org/10.1002/wcc.652.

Garfinkel, C., Hartmann, D., 2008. Different ENSO teleconnections and their effects on the stratospheric polar vortex. J. Geophys. Res.: Atmos. 113. https://doi.org/10.1029/2008JD009920.

Garfinkel, C.I., Gordon, A., Oman, L.D., Li, F., Davis, S., Pawson, S., 2018. Nonlinear response of tropical lower-stratospheric temperature and water vapor to ENSO. Atmos. Chem. Phys. 18, 4597-4615. https://doi.org/10.5194/acp-18-4597-2018.

Gettelman, A., Mills, M., Kinnison, D., Garcia, R., Smith, A., Marsh, D., Tilmes, S., Vitt, F., Bardeen, C., McInerny, J., 2019. The whole atmosphere community climate model version 6 (WACCM6). J. Geophys. Res.: Atmos. 124, 12380-12403. https://doi.org/10.1029/2019JD030943.
Hurwitz, M.M., Song, I.S., Oman, L.D., Newman, P.A., Molod, A.M., Frith, S.M., Nielsen, J.E., 2011. Response of the Antarctic stratosphere to warm pool El Niño Events in the GEOS CCM. Atmos. Chem. Phys. 11, 9659-9669. https://doi.org/10.5194/acp-11-9659-2011.
Jeong, Y., Kim, S.W., Kim, J., Shin, D., Kim, J., Park, J.H., An, S.I., 2023. Influence of ENSO on tropospheric ozone variability in East Asia. J. Geophys. Res.: Atmos. 128, e2023JD038604. https://doi.org/10.1029/2023JD038604.
Kawatani, Y., Hamilton, K., Sato, K., Dunkerton, T.J., Watanabe, S., Kikuchi, K., 2019. ENSO modulation of the QBO: Results from MIROC models with and without nonorographic gravity wave parameterization. J. Atmos. Sci. 76, 3893-3917. https://doi.org/10.1175/JAS-D-19-0163.1.
Kessenich, H.E., Seppälä, A., Rodger, C.J., 2023. Potential drivers of the recent large Antarctic ozone holes. Nat. Commun. 14, 7259. https://doi.org/10.1038/s41467-023-42637-0.
Kuttippurath, J., Lefèvre, F., Pommereau, J.P., Roscoe, H.K., Goutail, F., Pazmiño, A., Shanklin, J.D., 2013. Antarctic ozone loss in 1979–2010: first sign of ozone recovery. Atmos. Chem. Phys. 13, 1625-1635. https://doi.org/10.5194/acp-13-1625-2013.
Kuttippurath, J., Nair, P.J., 2017. The signs of Antarctic ozone hole recovery. Sci. Rep. 7, 585. https://doi.org/10.1038/s41598-017-00722-7.
Li, Y., Dhomse, S.S., Chipperfield, M.P., Feng, W., Bian, J., Xia, Y., Guo, D., 2023. Quantifying stratospheric ozone trends over 1984–2020: a comparison of ordinary and regularized multivariate regression models. Atmos. Chem. Phys. 23, 13029-13047. https://doi.org/10.5194/acp-23-13029-2023.
Li, Y., Xu, F., Wan, L., Chen, P., Guo, D., Chang, S., Yang, C., 2023. Effect of ENSO on the Ozone Valley over the Tibetan Plateau Based on the WACCM4 Model. Remote Sens. 15, 525.
Lin, J., Qian, T., 2019. Impacts of the ENSO lifecycle on stratospheric ozone and temperature. Geophys. Res. Lett. 46, 10646-10658. https://doi.org/10.1029/2019GL083697.
Livesey, N., Filipiak, M., Froidevaux, L., Read, W., Lambert, A., Santee, M., Jiang, J., Pumphrey, H., Waters, J., Cofield, R., 2008. Validation of Aura Microwave Limb Sounder O3 and CO observations in the upper troposphere and lower stratosphere. J. Geophys. Res.: Atmos. 113. https://doi.org/10.1029/2007JD008805.
Newman, P.A., 2010. Chemistry and dynamics of the Antarctic ozone hole. The stratosphere: dynamics, transport, and chemistry. 190, 157-171.
Newman, P.A., Nash, E.R., Rosenfield, J.E., 2001. What controls the temperature of the Arctic stratosphere during the spring? J. Geophys. Res.: Atmos. 106, 19999-20010. https://doi.org/10.1029/2000JD000061.
Niu, Y., Xie, F., Wu, S., 2023. ENSO modoki impacts on the interannual variations of spring Antarctic stratospheric ozone. J. Clim. 36, 5641-5658.

https://doi.org/10.1175/JCLI-D-22-0826.1.
Oman, L.D., Douglass, A.R., Ziemke, J.R., Rodriguez, J.M., Waugh, D.W., Nielsen, J.E., 2013. The ozone response to ENSO in Aura satellite measurements and a chemistry-climate simulation. J. Geophys. Res.: Atmos. 118, 965-976. https://doi.org/10.1029/2012JD018546.
Orr, A., Bracegirdle, T.J., Hosking, J.S., Feng, W., Roscoe, H.K., Haigh, J.D., 2012. Strong dynamical modulation of the cooling of the polar stratosphere associated with the Antarctic ozone hole. J. Clim. 26, 662-668. https://doi.org/10.1175/JCLI-D-12-00480.1.
Polvani, L.M., Waugh, D.W., Correa, G.J., Son, S.-W., 2011. Stratospheric ozone depletion: The main driver of twentieth-century atmospheric circulation changes in the Southern Hemisphere. J. Clim. 24, 795-812. https://doi.org/10.1175/2010JCLI3772.1.
Rao, J., Garfinkel, C.I., White, I.P., Schwartz, C., 2020. The Southern Hemisphere Minor Sudden Stratospheric Warming in September 2019 and its Predictions in S2S Models. J. Geophys. Res.: Atmos. 125. https://doi.org/10.1029/2020jd032723.
Rao, J., Ren, R., 2020. Modeling study of the destructive interference between the tropical Indian Ocean and eastern Pacific in their forcing in the southern winter extratropical stratosphere during ENSO. Clim. Dyn. 54, 2249-2266. https://doi.org/10.1007/s00382-019-05111-6.
Roy, R., Kumar, P., Kuttippurath, J., Lefevre, F., 2024. Chemical ozone loss and chlorine activation in the Antarctic winters of 2013–2020. Atmos. Chem. Phys. 24, 2377-2386. https://doi.org/10.5194/acp-24-2377-2024.
Sheng, Z., He, Y., Wang, S., Chang, S., Leng, H., Wang, J., Zhang, J., Wang, Y., Zhang, H., Sui, H., Song, Y., Wu, G., Guo, S., Chai, J., Feng, W., Song, J., 2025. Dynamics, chemistry, and modelling studies in the aviation and aerospace transition zones. The Innovation. https://doi.org/10.1016/j.xinn.2025.101012.
Sigmond, M., Shepherd, T.G., Simpson, I.R., 2011. Dynamics of the Lower Stratospheric Circulation Response to ENSO. J. Atmos. Sci. 68, 2537-2556. https://doi.org/10.1175/jas-d-11-05.1.
Solomon, S., 1999. Stratospheric ozone depletion: A review of concepts and history[J]. Rev. Geophys. 37, 275-316. https://doi.org/10.1029/1999rg900008.
Solomon, S., Ivy, D.J., Kinnison, D., Mills, M.J., Neely III, R.R., Schmidt, A., 2016. Emergence of healing in the Antarctic ozone layer. Science. 353, 269-274. https://doi.org/10.1126/science.aae0061.
Stone, K.A., Solomon, S., Thompson, D.W., Kinnison, D.E., Fyfe, J.C., 2022. On the Southern Hemisphere stratospheric response to ENSO and its impacts on tropospheric circulation. J. Clim. 35, 1963-1981. https://doi.org/10.1175/JCLI-D-21-0250.1.
Szeląg, M.E., Sofieva, V.F., Degenstein, D., Roth, C., Davis, S., Froidevaux, L., 2020. Seasonal stratospheric ozone trends over 2000–2018 derived from several merged data sets. Atmos. Chem. Phys. 20, 7035-7047. https://doi.org/10.5194/acp-20-7035-2020.
Tung, K.-K., Ko, M.K., Rodriguez, J.M., Dak Sze, N., 1986. Are Antarctic ozone variations a manifestation of dynamics or chemistry? Nature. 322, 811-814. https://doi.org/10.1038/322811a0.
Wang, H., Rao, J., Guo, D., Liu, Y., Lu, Y., 2024a. A revisit of the linearity in the

combined effect of ENSO and QBO on the stratosphere: model evidence from CMIP5/6. Clim. Dyn. 62, 9633-9650. https://doi.org/10.1007/s00382-024-07430-9.
Wang, H., Rao, J., Guo, D., Lu, Y., Liu, Y., 2024b. Linear interference between effects of ENSO and QBO on the northern winter stratospheric polar vortex. Clim. Dyn. 62, 2925-2940. https://doi.org/10.1007/s00382-023-07040-x.
Wang, J., Pawson, S., Tian, B., Liang, M.-C., Shia, R.-L., Yung, Y.L., Jiang, X., 2011. El Niño–Southern Oscillation in tropical and midlatitude column ozone. J. Atmos. Sci. 68, 1911-1921. https://doi.org/10.1175/JAS-D-11-045.1.
Weber, M., Arosio, C., Coldewey-Egbers, M., Fioletov, V.E., Frith, S.M., Wild, J.D., Tourpali, K., Burrows, J.P., Loyola, D., 2022. Global total ozone recovery trends attributed to ozone-depleting substance (ODS) changes derived from five merged ozone datasets. Atmos. Chem. Phys. 22, 6843-6859. https://doi.org/10.5194/acp-22-6843-2022.
Weber, M., Dikty, S., Burrows, J.P., Garny, H., Dameris, M., Kubin, A., Abalichin, J., Langematz, U., 2011. The Brewer-Dobson circulation and total ozone from seasonal to decadal time scales. Atmos. Chem. Phys. 11, 11221-11235. https://doi.org/10.5194/acp-11-11221-2011.
WMO, 2022. Scientific Assessment of Ozone Depletion: 2022. Global Ozone Research and Monitoring Project-Report No. 278. Geneva, Switzerland.
Xie, F., Li, J., Tian, W., Feng, J., Huo, Y., 2012. Signals of El Niño Modoki in the tropical tropopause layer and stratosphere. Atmos. Chem. Phys. 12, 5259-5273. https://doi.org/10.5194/acp-12-5259-2012.
Xie, F., Li, J., Tian, W., Zhang, J., Shu, J., 2014. The impacts of two types of El Niño on global ozone variations in the last three decades. Adv. Atmos. Sci. 31, 1113-1126. https://doi.org/10.1007/s00376-013-3166-0.
Yang, C., Li, T., Dou, X., Xue, X., 2015. Signal of central Pacific El Niño in the Southern Hemispheric stratosphere during austral spring. J. Geophys. Res.: Atmos. 120, 11,438-411,450. https://doi.org/10.1002/2015JD023486.
Yook, S., Thompson, D.W., Solomon, S., 2022. Climate impacts and potential drivers of the unprecedented Antarctic ozone holes of 2020 and 2021. Geophys. Res. Lett. 49, e2022GL098064. https://doi.org/10.1029/2022GL098064.
Zhang, J., Tian, W., Wang, Z., Xie, F., Wang, F., 2015. The influence of ENSO on northern midlatitude ozone during the winter to spring transition. J. Clim. 28, 4774-4793. https://doi.org/10.1175/JCLI-D-14-00615.1.
Zhang, J., Zhang, C., Zhang, K., Xu, M., Duan, J., Chipperfield, M.P., Feng, W., Zhao, S., Xie, F., 2021. The role of chemical processes in the quasi-biennial oscillation (QBO) signal in stratospheric ozone. Atmos. Environ. 244, 117906. https://doi.org/10.1016/j.atmosenv.2020.117906.
Zhou, T., DallaSanta, K.J., Orbe, C., Rind, D.H., Jonas, J.A., Nazarenko, L., Schmidt, G.A., Russell, G., 2024. Exploring the ENSO modulation of the QBO periods with GISS E2. 2 models. Atmos. Chem. Phys. 24, 509-532. https://doi.org/10.5194/acp-24-509-2024.
Zhou, X., Dhomse, S.S., Feng, W., Mann, G., Heddell, S., Pumphrey, H., Kerridge, B.J., Latter, B., Siddans, R., Ventress, L., Querel, R., Smale, P., Asher, E., Hall, E.G., Bekki,

S., Chipperfield, M.P., 2024. Antarctic Vortex Dehydration in 2023 as a Substantial Removal Pathway for Hunga Tonga-Hunga Ha'apai Water Vapor. Geophys. Res. Lett. 51, e2023GL107630. https://doi.org/10.1029/2023gl107630.

Declaration of interests

☒The authors declare that they have no known competing financial interests or personal relationships that could have appeared to influence the work reported in this paper.

☐The authors declare the following financial interests/personal relationships which may be considered as potential competing interests:

CRediT authorship contribution statement

Haotian He: Writing – review & editing, Writing – original draft, Data curation, Methodology, Visualization, Investigation, Formal analysis. Shujie Chang: Writing – review & editing, Writing – original draft, Conceptualization, Methodology, Funding acquisition. Wuhu Feng: Writing – review & editing, Methodology, Supervision. Martyn P. Chipperfield: Writing – review & editing, Resources, Data curation, Supervision. Sandip S. Dhomse: Writing – review & editing. Yuwen Li: Writing – review & editing, Visualization. Saffron Heddell: Writing – review & editing.